

# Phosphatidylinositol 5-Kinase Stimulates Apical Biosynthetic Delivery via an Arp2/3-dependent Mechanism<sup>\*S</sup>

Received for publication, February 8, 2006, and in revised form, April 6, 2006 Published, JBC Papers in Press, April 6, 2006, DOI 10.1074/jbc.M601239200

Christopher J. Guerriero<sup>1</sup>, Kelly M. Weixel<sup>1</sup>, Jennifer R. Bruns, and Ora A. Weisz<sup>2</sup>

From the Laboratory of Epithelial Cell Biology, Renal-Electrolyte Division, University of Pittsburgh, Pittsburgh, Pennsylvania 15261

The mechanisms by which polarized epithelial cells target distinct carriers enriched in newly synthesized proteins to the apical or basolateral membrane remain largely unknown. Here we investigated the effect of phosphatidylinositol metabolism and modulation of the actin cytoskeleton, two regulatory mechanisms that have individually been suggested to function in biosynthetic traffic, on polarized traffic in Madin-Darby canine kidney cells. Overexpression of phosphatidylinositol 5-kinase (PI5K) increased actin comet frequency in Madin-Darby canine kidney cells and concomitantly stimulated *trans*-Golgi network (TGN) to apical membrane delivery of the raft-associated protein influenza hemagglutinin (HA), but did not affect delivery of a non-raft-associated apical protein or a basolateral marker. Modulation of actin comet formation by pharmacologic means, by overexpression of the TGN-localized inositol polyphosphate 5-phosphatase Ocr1, or by blockade of Arp2/3 function had parallel effects on the rate of apical delivery of HA. Moreover, HA released from a TGN block was colocalized in transport carriers in association with PI5K and actin comets. Inhibition of Arp2/3 function in combination with microtubule depolymerization led to a virtual block in HA delivery, suggesting synergistic coordination of these cytoskeletal assemblies in membrane transport. Our results suggest a previously unidentified role for actin comet-mediated propulsion in the biosynthetic delivery of a subset of apical proteins.

The maintenance of polarized cell function requires continuous active sorting and delivery of newly synthesized proteins and lipids to differentiated apical and basolateral plasma membrane domains. Tight junctions between the cells prevent the diffusion of surface proteins between these domains, but polarity is established and maintained largely by the selective delivery and recycling of proteins to their appropriate site of function. In polarized renal cells, it is thought that newly synthesized proteins are sorted initially at the *trans*-Golgi network (TGN)<sup>3</sup> into distinct carriers destined for the apical or basolateral domain (1, 2). Transport of some proteins to their ultimate destination may be indirect and include passage through endosomal compartments or the opposite surface domain (2).

The sorting of individual proteins to the apical and basolateral cell surface domains is signal-mediated. Basolateral sorting signals generally reside in the cytoplasmically disposed regions of proteins, whereas glycan-, lipid-, and peptide-dependent signals have been identified that reside in the luminal, membrane-associated, or cytoplasmic regions of distinct apically targeted proteins (2). Little is known about how the sorting machinery recognizes these diverse signals; however, a current model suggests that preferential incorporation of a subset of apical proteins, including those with glycosphingolipid anchors or sorting signals within their transmembrane domains, into glycolipid-enriched microdomains (lipid rafts) is important for their polarized delivery (1). Interestingly, apical delivery of raft *versus* non-raft proteins may involve distinct transport carriers that are independently regulated (3, 4).

There is increasing evidence for a role of phosphatidylinositols in the regulation of biosynthetic membrane traffic (5). The Golgi contains a sizable pool of phosphatidylinositol 4-phosphate (PI4P) and harbors two PI4P-synthesizing enzymes (PI4KIII $\beta$  and PI4KII $\alpha$  (6–9)). Our laboratory has previously demonstrated that overexpression of PI4KIII $\beta$  inhibits the rate of apical membrane delivery of the raft-associated protein influenza hemagglutinin (HA), whereas expression of a kinase-deficient mutant stimulates delivery (8). However, it is conceivable that these effects are due to a downstream metabolite of PI4P, such as phosphatidylinositol 4,5-bisphosphate (PIP<sub>2</sub>). Indeed, although there is only a small amount of this lipid that can be visualized in the Golgi complex (10), PIP<sub>2</sub> is readily generated on isolated Golgi membranes incubated with phosphatidylinositol 4-phosphate 5-kinases (PI5Ks (11)) and several possible functions for PIP<sub>2</sub> in biosynthetic membrane traffic have been postulated (5, 12, 13). Additionally, the presence of Ocr1, a TGN-localized PIP<sub>2</sub> 5'-phosphatase that is defective or absent in patients with oculocerebrorenal syndrome of Lowe, lends further support to a role for PIP<sub>2</sub> metabolism in that compartment (14, 15).

Increases in PIP<sub>2</sub> levels upon expression of PI5Ks leads to production of rapidly nucleating branches of actin filaments, termed actin comets, which are capable of propelling transport vesicles through the cytoplasm (16). Neuronal Wiskott-Aldrich syndrome protein (N-WASP), a potent stimulator of actin nucleation via the Arp2/3 complex, is activated by PIP<sub>2</sub> and transduces elevated PIP<sub>2</sub> levels into an increased frequency of actin comets (17). N-WASP and Arp2/3 are localized to the Golgi complex (among other sites), and a link between actin comets and biosynthetic traffic has been previously suggested (18). However, the effects of manipulating PI5K or Arp2/3 activity on the fidelity or rate of biosynthetic transport have not been explored.

Here we have examined the effect of increasing PIP<sub>2</sub> synthesis on polarized biosynthetic traffic in Madin-Darby canine kidney (MDCK) cells. Expression of PI5K selectively stimulated the TGN to apical delivery of a raft-associated protein without affecting the overall polarity of delivery. Moreover, the effect of PIP<sub>2</sub> appears to involve an Arp2/3-dependent pathway, as a dominant-negative inhibitor of Arp2/3 function selectively inhibited biosynthetic transport of this protein. MDCK cells overexpressing PI5K had markedly increased numbers of actin comets,

\* This work was supported in part by National Institutes of Health Grants DK054407 and DK064613 and the Commonwealth of Pennsylvania (to O. A. W.). The costs of publication of this article were defrayed in part by the payment of page charges. This article must therefore be hereby marked "advertisement" in accordance with 18 U.S.C. Section 1734 solely to indicate this fact.

<sup>S</sup> The on-line version of this article (available at <http://www.jbc.org>) contains supplemental Movie 1.

<sup>1</sup> Supported in part by National Institutes of Health Grant T32-DK61296.

<sup>2</sup> To whom correspondence should be addressed: 3550 Terrace St., Pittsburgh, PA 15261. Tel.: 412-383-8891; Fax: 412-383-8956; E-mail: [weisz@pitt.edu](mailto:weisz@pitt.edu).

<sup>3</sup> The abbreviations used are: TGN, *trans*-Golgi network; AV, adenovirus; DOX, doxycycline; endo H, endoglycosidase H; HA, hemagglutinin; MDCK, Madin-Darby canine kidney; m.o.i., multiplicity of infection; N-WASP, neuronal Wiskott-Aldrich syndrome protein; PI5K, human phosphatidylinositol 5-kinase  $\alpha$  isoform; PMA, phorbol myristate acetate; PI4P, phosphatidylinositol 4-phosphate; PIP<sub>2</sub>, phosphatidylinositol 4,5-bisphosphate; VSV, vesicular stomatitis virus; PBS, phosphate-buffered saline.

and HA could be visualized at the tips of these structures. Disruption of actin comet formation together with microtubule depolymerization led to a nearly total blockade in apical delivery, suggesting a concerted role of these distinct cytoskeletal assemblies for efficient and polarized apical transport. Our data suggest that actin comets contribute selectively to the polarized delivery of apically destined transport containers enriched in lipid raft-associated cargo.

## EXPERIMENTAL PROCEDURES

**DNA and Replication-defective Recombinant Adenoviruses**—The  $\alpha$  isoform of murine phosphatidylinositol 5-kinase (PI5K) cloned into the pAdtet vector was provided by Andreas Jeromin (Baylor University). Constructs encoding *myc*-tagged W and WA domains of WAVE1 were generous gifts of Dr. Dorothy Schafer and Dr. James Casanova (University of Virginia). Fluorescent protein-tagged actin constructs were provided by Dr. Ronald Montelaro (University of Pittsburgh). The generation and purification of replication-defective recombinant adenoviruses (AVs) encoding tetracycline-repressible influenza HA (Japan serotype), vesicular stomatitis virus G protein (VSV-G), and a control virus (encoding the influenza Rostock M2 coding sequence in the reverse orientation) has been previously described (8, 19). AVs encoding PI5K, and human Ocrl (both wild type and the phosphatase-deficient mutant R483G; constructs provided by Dr. Robert Nussbaum, National Institutes of Health) were generated using similar methods. AV encoding p75<sup>NTR</sup> was provided by Dr. Enrique Rodriguez-Boulan (Weill Medical College) with permission from Dr. Moses Chao, and AV-W and WA were kind gifts of Dr. James Casanova (University of Virginia).

**Cell Lines and Adenoviral Infection**—MDCK type II cells stably expressing tetracycline transactivator were cultured in modified Eagle's medium (Sigma) supplemented with 10% fetal bovine serum. For measurements of intra-Golgi transport, kinetics of surface delivery, and surface polarity, cells were seeded at superconfluence in 12-mm transwells (0.4- $\mu$ m pore; Costar, Cambridge, MA) for 2–4 days prior to infection with recombinant AVs at the following multiplicity of infection (m.o.i.) (control AV, AV-PI5K, AV-W, and AV-WA, m.o.i. 100–250; AV-HA, AV-p75, and AV-VSV-G, m.o.i. 25–50) as described in Ref. 19. Experiments were performed the following day.

**Indirect Immunofluorescence**—MDCK cells grown on transwell filters or coverslips were infected with AVs at the indicated m.o.i. The following day, cells were rinsed once with PBS, fixed in 3.7% formaldehyde, rinsed with PBS containing 10 mM glycine (PBS-G), then permeabilized with 0.5% Triton X-100 in PBS-G for 3 min at room temperature. After washing, nonspecific binding sites were blocked by incubation for 5 min in PBS-G containing 0.25% (w/v) ovalbumin. Coverslips were incubated for 30 min with monoclonal anti-HA tag antibody (1:500 dilution; Covance) followed by washing in blocking buffer. Cells were then incubated for 30 min with secondary antibodies Alexa Fluor goat anti-mouse 488 (1:500; Invitrogen, Carlsbad, CA). Rhodamine phalloidin (1:80; Invitrogen) was included in this step where indicated. After extensive washing, coverslips or filters were mounted onto slides. Filter-grown MDCK cells were fixed with formaldehyde using a pH-shift protocol and processed as described in Ref. 20. Images were captured using a Leica TCS-SL confocal microscope equipped with argon and green and red helium neon lasers (Leica, Dearfield, IL). Images were taken with a  $\times 100$  (1.4 numerical aperture) plan apochromat oil objective. TIFF images were processed using Adobe Photoshop (Adobe, San Jose, CA).

**Intracellular Transport and Cell Surface Delivery Assays**—AV-infected filter-grown MDCK cells were starved for 30 min and radiolabeled for 5–10 min (endoglycosidase H (endo H) kinetics) or 15–20 min

(TGN to surface delivery) with 1 mCi/ml Tran-<sup>35</sup>S-label® (MP Bio-medicals, Irvine, CA). To measure endo H kinetics, cells were chased in bicarbonate-free modified Eagle's medium for the indicated periods, solubilized, and HA immunoprecipitated as previously described in Ref. 19. After collection of antibody-antigen complexes, samples were eluted, divided in half, and mock-treated or treated overnight with endo H prior to electrophoresis on 10% SDS-PAGE gels. To measure TGN to surface delivery, radiolabeled cells were chased at 19 °C for 2 h unless otherwise indicated to stage newly synthesized membrane proteins in the TGN. The cells were then rapidly warmed to 32 or 37 °C as indicated. Apical delivery of HA was measured by trypsinization as described in Ref. 21. Basolateral delivery of VSV-G was quantitated using domain selective biotinylation as described in Ref. 22. To quantitate surface delivery of p75<sup>NTR</sup>, cells were radiolabeled on 25- $\mu$ l drops of sulfate-free medium containing 100  $\mu$ Ci of [<sup>35</sup>S]sulfate at 18 °C and the rate of surface delivery was assessed using domain selective biotinylation upon subsequent warmup to 37 °C (23). Immunoprecipitation of HA, VSV-G, or p75 was performed using supernatants from cultured hybridomas (Fc125 from Dr. Thomas Braciale, University of Virginia; 8G5 from Dr. Douglas Lyles, Wake Forest University (24); and MA 20.1 from Dr. Enrique Rodriguez-Boulan, Weill Medical College, respectively).

**Visualization and Quantitation of Actin Comets**—MDCK cells ( $2 \times 10^5$ ) were seeded on Biotech 0.17-mm  $\Delta$ T dishes (Biotech Inc., Butler, PA). The following day cells were infected with AVs (m.o.i. 100–250) encoding the indicated proteins, and incubated overnight with 0.25 ng/ml doxycycline (DOX) to partially suppress protein expression. The following morning DOX was removed by thorough washing. Cells were then pressure-injected with cDNA encoding GFP- or YFP-actin and were returned to culture for 5 h. Following that time the cells were imaged on an Olympus IX81 microscope using a  $\times 100$  Olympus UPlanApo objective (numerical aperture 1.35). Random fields containing fluorescent actin-expressing cells were imaged every 2 s for 4 min. Data were analyzed using acquisition software (Slidebook) to determine the percentage of cells with comets. Stable cell lines expressing fluorescent protein-tagged actin were generated using Lipofectamine 2000 and mixed populations were isolated by selection in G418. These cells were infected with AV-PI5K where indicated and used for the quantification of actin comets in cells treated with phorbol myristate acetate (PMA; 5  $\mu$ g/ml), cytochalasin D (25  $\mu$ g/ml), 1-butanol (1% v/v), and *t*-butyl alcohol (1% v/v).

**Visualization of Cargo Associated with Actin Comets**—MDCK cells ( $3 \times 10^5$ ) were seeded onto coverslips in 12-well dishes. The following day the cells were co-infected with AVs encoding HA and either PI5K or control AV. After 8 h at 37 °C, the cells were incubated at 19 °C for 2.5 h to stage HA in the TGN. Dishes were then warmed to 37 °C for 0 or 30 min before fixation and processing for indirect immunofluorescence to detect HA, PI5K, and actin.

## RESULTS

**PI5K Selectively Stimulates Biosynthetic Delivery of an Apical Raft-associated Protein**—We examined the effect of AV-mediated overexpression of murine PI5K $\alpha$  on biosynthetic traffic in polarized MDCK cells. Overexpression of PI5K increased cellular levels of PIP<sub>2</sub> by 2–3-fold (not shown) but did not alter intra-Golgi kinetics based on the quantitation of the rate of acquisition of resistance to endo H digestion of influenza HA (Fig. 1A). To examine the effect of PI5K on the kinetics of post-Golgi transport, we staged newly synthesized radiolabeled HA in the TGN at 19 °C, and using a cell surface

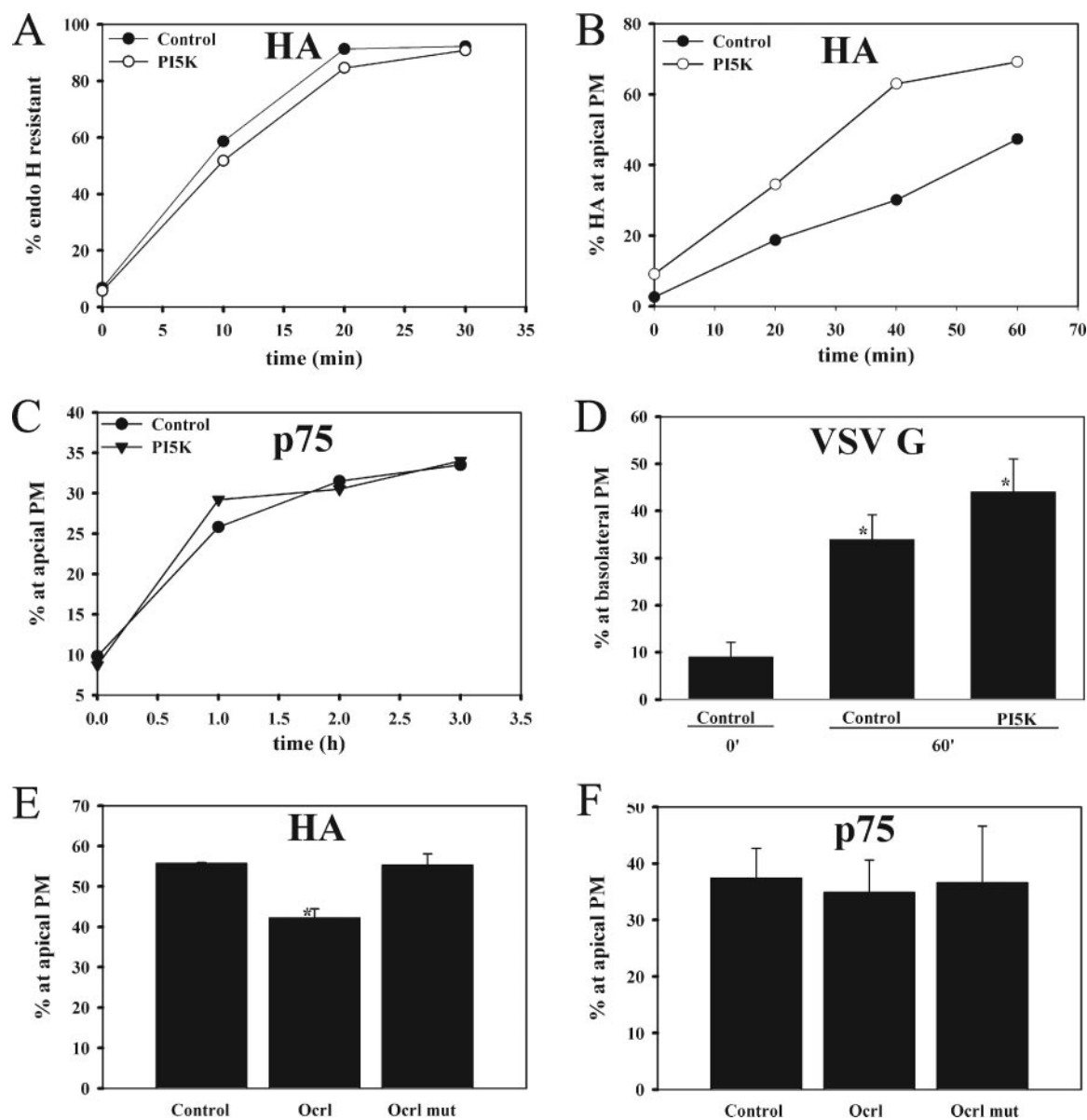


**FIGURE 1. TGN to apical membrane delivery of a raft-associated protein is selectively modulated by PI5K and Ocr1.** A, filter-grown MDCK cells co-infected with AV-HA and either control AV or AV-PI5K were starved, radiolabeled for 5 min, and chased at 37 °C for the indicated time periods. HA was immunoprecipitated from cell lysates, the samples were treated with endo H, and the fraction of HA that was resistant to endo H at each time point was quantitated. Similar results were obtained in three experiments. B, MDCK cells co-infected with AV-HA and either control AV or AV-PI5K were radiolabeled for 15 min and chased for 2 h at 19 °C. Apical delivery of HA was quantitated by cell surface trypsinization at various times after warming to 37 °C. Similar results were obtained in 13 experiments comparing HA transport in control and PI5K-expressing cells. C, MDCK cells co-infected with AV-p75 and either control AV or AV-PI5K were radiolabeled for 2 h at 18 °C with [<sup>35</sup>S]sulfate prior to warming to 37 °C for the indicated times. Apical delivery of p75 was quantitated by domain selective biotinylation. Similar results were obtained in three independent experiments. D, MDCK cells co-infected with AV-VSV-G and either control AV or AV-PI5K were radiolabeled and then chased for 2 h at 19 °C prior to warming to 37 °C for 0 or 60 min. Basolateral delivery was quantitated by domain selective biotinylation. The mean ± S.E. of the indicated number of experiments performed in triplicate or quadruplicate is plotted;  $n = 3$  for 0 min;  $n \geq 4$  for 60 min. \*,  $p \leq 0.02$  versus control at 0 min. MDCK cells co-infected with AV-HA (E) or AV-p75 (F) and either control AV or AVs expressing wild type or kinase-deficient Ocr1 were starved in sulfate-free media for 30 min and radiolabeled for 2.5 h at 18 °C with [<sup>35</sup>S]sulfate prior to warming to 37 °C. Apical delivery of HA (at 1 h) was quantified using cell surface trypsinization; delivery of p75 (at 2 h) was quantitated by domain selective biotinylation. The percent delivery (mean ± S.E.) of HA ( $n = 3$ ) and p75 ( $n = 5-6$ ) is shown. \* denotes statistical significance from control measured using Student's *t* test ( $p = 0.004$ ).

trypsinization assay measured the rate of its delivery to the apical cell surface upon warming to 37 °C. Roughly 50% of the total HA expressed in control cells reached the apical membrane within 1 h (Fig. 1B). In contrast, HA delivery was markedly stimulated in cells overexpressing PI5K (~67% at 1 h).

We next examined the effect of PI5K on the TGN to surface transport kinetics of p75, an apical marker not known to associate with lipid rafts in MDCK cells (Fig. 1C), as well as on the basolateral marker VSV-G (Fig. 1D). PI5K had no effect on the biosynthetic delivery of either of these proteins. Thus, the stimulatory effect of PI5K on surface delivery appears to be selective for raft-associated proteins.

*Overexpression of Ocr1 Selectively Inhibits Biosynthetic Delivery of Influenza HA*—To examine whether stimulation of PIP<sub>2</sub> synthesis in the TGN was responsible for the stimulatory effect of PI5K, we compared the effect of overexpressing the TGN-localized PIP<sub>2</sub> 5'-phosphatase Ocr1 (or as a control, expressing a phosphatase-deficient mutant of Ocr1) on the delivery of HA and p75. Because overexpression of both wild type and mutant Ocr1 slowed intra-Golgi transport as assessed by monitoring endo H kinetics, we used [<sup>35</sup>S]sulfate to selectively radiolabel proteins in the TGN. As shown in Fig. 1E, expression of wild type Ocr1 inhibited TGN to apical delivery of HA, whereas mutant Ocr1 had no effect. Consistent with the selective effect of PI5K on HA delivery,

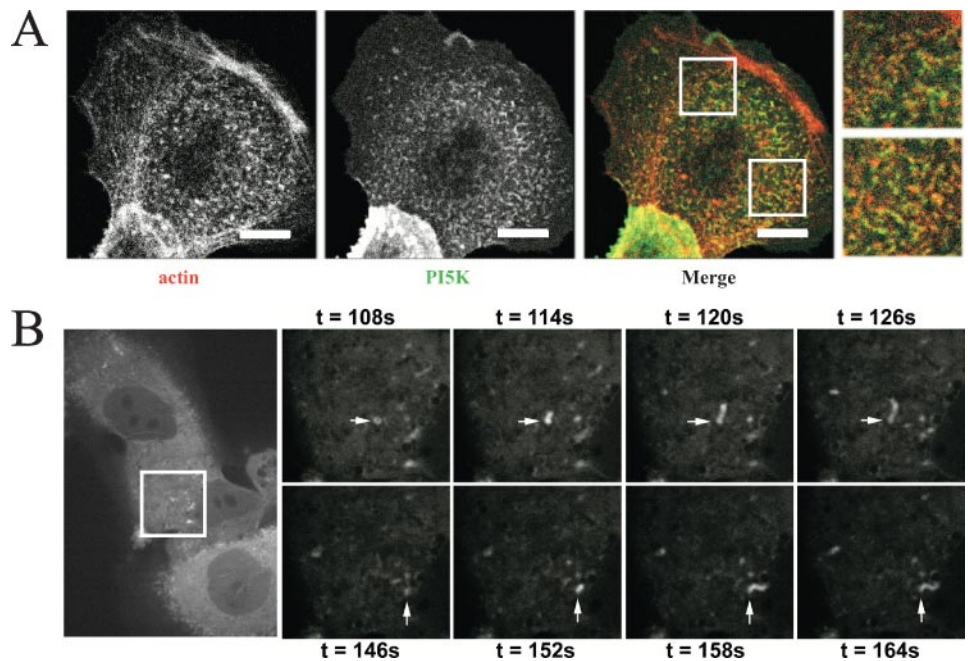


**FIGURE 2. PI5K localizes to actin filaments and stimulates actin comet formation in MDCK cells.** A, MDCK cells seeded on coverslips were infected with AV-PI5K and processed for indirect immunofluorescence the following day to detect actin (with rhodamine phalloidin) and the PI5K HA epitope tag (visualized using Alexa 488-conjugated goat anti-mouse secondary antibody). Individual confocal sections and a merged image are shown. The enlarged insets highlight areas where colocalization of PI5K with short actin filaments is clearly evident. Scale bar, 7.5  $\mu\text{m}$ . B, MDCK cells stably expressing GFP-actin were infected with AV-PI5K for 6 h and then imaged every 2 s. Enlarged areas shown are from individual frames from the supplementary movie. Two comets are seen to initiate from the area highlighted by the square over the time course; one at 108 s, and the other at 146 s. The starting points for each comet are marked with white arrowheads in subsequent frames.

**TABLE 1**  
**Quantitation of actin comet frequency in MDCK cells**

MDCK cells seeded onto Biotec 0.17-mm  $\Delta\text{T}$  dishes were infected with either control AV or AVs encoding WA, PI5K, or Ocr1 (m.o.i. 100–250). The samples were kept in 0.25 ng/ml DOX overnight to suppress protein expression from the AVs. The next day, DOX was thoroughly washed out and cells were microinjected with cDNA encoding GFP-actin and random fields were imaged for 4-min intervals starting 5 h later. The effects of PMA on actin comets were quantitated using MDCK cells stably expressing GFP-actin. Actin comets in cytochalasin D (cyto D) and 1-butanol-treated cells were imaged using MDCK cells stably expressing GFP-actin and infected with AV-PI5K for 8 h, and comet formation was confirmed before addition of drug.

Condition	No. of cells imaged	Cells with comets
		%
Control	27	7.4
WA	10	0
PI5K	212	26.9
WA + PI5K	44	0
PMA	33	31.4
PI5K + cyto D	10	0
PI5K + 1-butanol	15	6.7
PI5K + Ocr1	47	0

neither wild type nor mutant Ocr1 affected the kinetics of p75 delivery (Fig. 1F).

**PI5K Stimulates the Formation of Actin Comets in MDCK Cells**—Because PI5K-mediated actin comets have been implicated in the transport of raft-associated proteins (18), we asked whether actin comet-mediated propulsion of HA transport carriers could be responsible for the stimulated surface delivery we observed. First, we sought to determine the relationship between PI5K and actin in fixed cells. MDCK cells were infected with AV expressing PI5K, then fixed and processed for indirect immunofluorescence 16 h later. Actin filaments were visualized using rhodamine phalloidin and the HA epitope tag on PI5K was detected using a monoclonal mouse antibody. PI5K colocalized extensively with actin filaments in confocal sections of MDCK cells (Fig. 2A). This is consistent with previous reports that PI5K is found in actin-rich fractions isolated from thrombin-activated platelets (25). Next, we used a live cell approach to determine whether PI5K stimulates the formation of actin comets. Actin comets have not previously been reported in MDCK cells. MDCK cells were seeded on glass coverslips, infected with AV encoding PI5K or control AV, and then incubated in the presence of

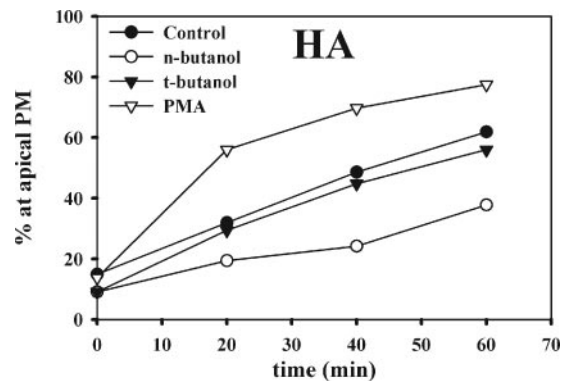


**FIGURE 3. PMA and 1-butanol have opposing effects on HA delivery.** MDCK cells infected with AV-HA were radiolabeled for 15 min and chased for 2 h at 19 °C. PMA (5  $\mu\text{g}/\text{ml}$  PMA), 1-butanol (n-butanol; 1% v/v), or t-butyl alcohol (t-butanol; 1% v/v) were added as indicated 10 min prior to the end of the chase period and included upon subsequent incubation at 37 °C for the indicated times. HA delivery to the apical surface was measured by cell surface trypsinization. Similar results were obtained in at least three experiments for each condition.

0.25 ng/ml DOX to suppress PI5K expression. The following day, the DOX was washed out and cells were microinjected with cDNA encoding GFP-actin. Random fields were imaged 5 h later for 4-min intervals using an Olympus IX81 equipped with a  $\times 100$  Olympus UPlanApo objective. Actin comets were defined as rapidly moving bursts of actin followed by a fading tail of presumably depolymerizing actin. Comets generated in MDCK cells were distinct but generally smaller than comets described by others using different cell lines, which have been reported to be up to 5  $\mu\text{m}$  in length (18, 26, 27). Comets were observed in 7% of control cells and in 27% of the cells overexpressing PI5K (Table 1, Fig. 2B, and supplementary movie).

Additionally, we were able to increase the frequency of actin comet formation in control cells by addition of the protein kinase C activator PMA, which has been previously demonstrated to stimulate actin comets *in vivo* (Table 1) (16). PMA also stimulated the rate of apical delivery of HA to an extent comparable with that observed upon overexpression of PI5K (Fig. 3). Conversely, addition of 1-butanol, which disrupts phospholipase D-mediated synthesis of the PI5K activator phosphatidic acid, profoundly inhibited the formation of PI5K-stimulated actin comets

## Actin Comet-mediated Apical Transport

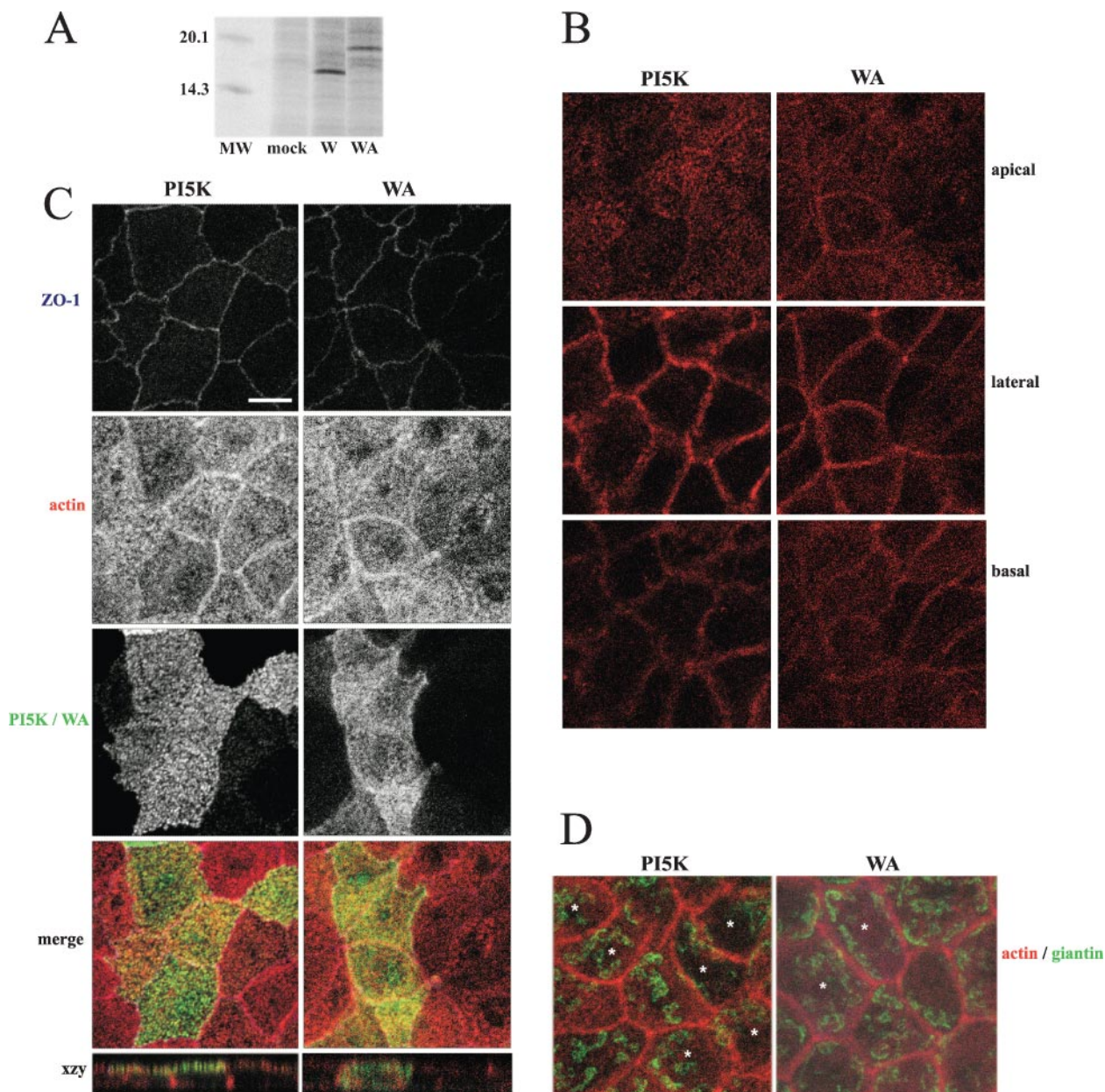


**FIGURE 4. Expression of PI5K or the WA domain of Scar1 does not alter Golgi or actin morphology.** *A*, MDCK cells were mock-infected or infected with AVs encoding the W or WA domain of Scar1, radiolabeled for 1 h, and lysates run on a 15% SDS gel. The positions of molecular weight markers (*MW*) are shown. W and WA migrate at their expected molecular masses (16 and 18 kDa, respectively). *B*, expression of PI5K or WA does not disrupt actin morphology in polarized MDCK cells. Confocal sections from the apical, lateral, and basal portions of rhodamine phalloidin-labeled PI5K- or WA-expressing cells are shown. *C*, expression of PI5K or WA does not alter tight junction morphology of MDCK cells. Filter-grown cells were infected with either PI5K- or WA-expressing AVs. Samples were fixed and processed for indirect immunofluorescence to detect ZO-1, and PI5K or WA. ZO-1 was detected using secondary antibody coupled to Alexa 647 and PI5K or WA was visualized using Alexa 488-conjugated goat anti-mouse secondary antibody. Rhodamine phalloidin was included in the secondary antibody incubations to detect filamentous actin. Samples were imaged by confocal microscopy, and five slices (0.5  $\mu\text{m}$  apart) through the region of the tight junctions were overlaid to make a maximum projection. Individual projections and merged xyz and xzy images are shown. *D*, samples infected as in *B* were stained with rhodamine phalloidin and monoclonal anti-giantin antibody followed by Alexa 488-conjugated secondary antibody. A projection of five sections taken through the Golgi region is shown. AV-infected cells (*asterisks*) were identified by co-labeling to detect PI5K (*left panel*) or WA (*right panel*). Scale bar = 7.5  $\mu\text{m}$  for all xyz sections shown.

(Table 1) and also blocked delivery of TGN-staged HA to the apical surface (Fig. 3). 1-Butanol-mediated inhibition of phosphatidic acid synthesis has previously been implicated in the release of secretory vesicles from the TGN of endocrine cells (28). In contrast, *t*-butyl alcohol, which does not affect phosphatidic acid synthesis, had no effect on comet formation or HA delivery (Fig. 3).

*The Effect of PI5K on HA Delivery Is Mediated through Arp2/3*—If actin comets are involved in the TGN to apical membrane delivery of HA, then blockade of the N-WASP-Arp2/3-mediated actin polymerization would be expected to inhibit HA transport. The WA domain of WASP/WAVE family proteins provides the binding sites for actin

monomers and Arp2/3, and when expressed in isolation is a potent inhibitor of N-WASP function (18, 29). As a control, we expressed the W domain, which binds to actin monomers but not to Arp2/3 (29).

Infection of MDCK cells with AVs encoding W or WA yielded comparable levels of the expected protein products (W ~16 kDa; WA ~18 kDa; Fig. 4A). As expected, expression of WA abolished PI5K-mediated formation of actin comets, demonstrating effective inhibition of Arp2/3 function (Table 1). We next examined the effect of the WA domain and PI5K on the morphology of polarized, filter-grown MDCK cells. Neither the WA domain nor PI5K had any apparent effect on cytoskeletal organization in polarized cells (Fig. 4B; similar results for W domain, not

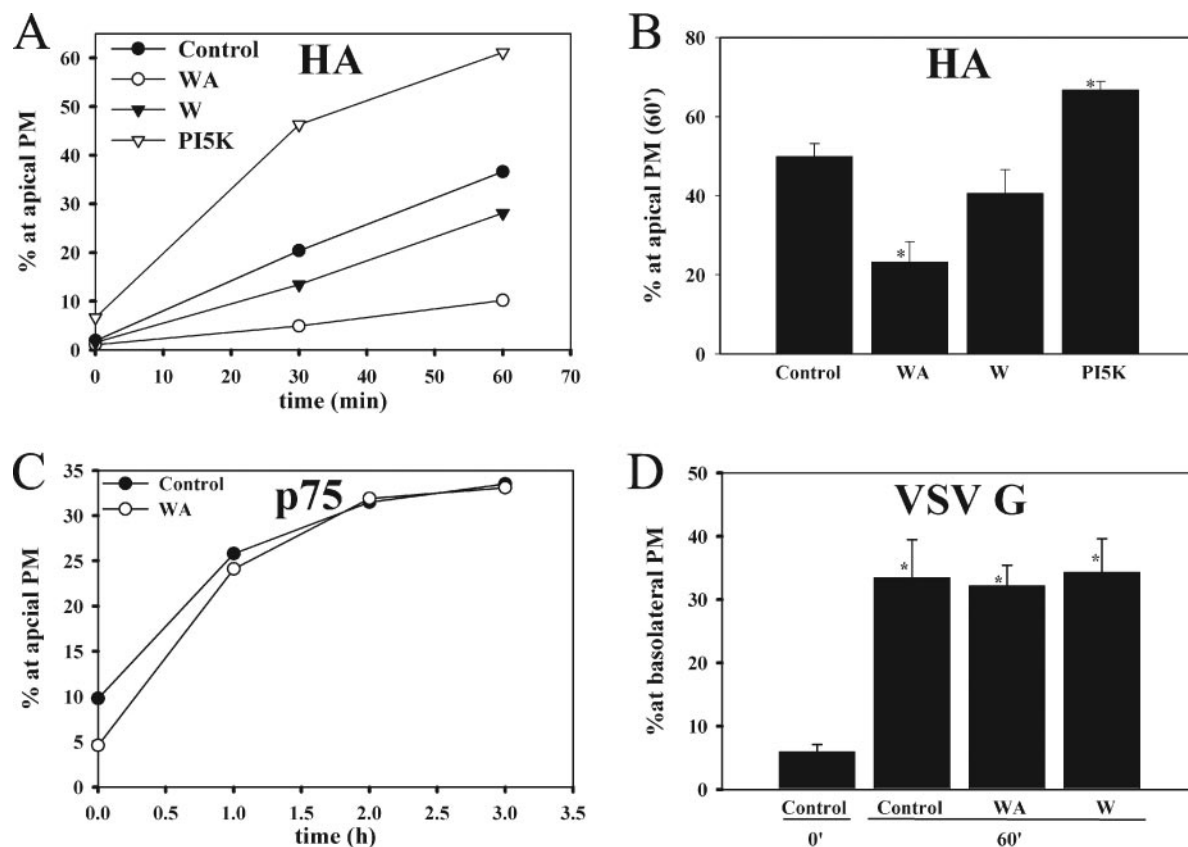


**FIGURE 5. Expression of WA selectively inhibits apical delivery of HA.** *A*, WA inhibits apical delivery of TGN-staged HA. The kinetics of HA surface delivery were quantitated in MDCK cells co-infected with AV-HA, and either control AV or WA-, W-, or PI5K-expressing AVs as described previously. *B*, quantitation of the effects of WA, W, and PI5K on HA delivery. The bar graph shows the mean % of total HA ( $\pm$  S.E.) at the apical surface after a 60-min chase in at least 8 experiments for each condition. \* denotes statistical significance from control measured using Student's *t* test (WA,  $n = 8$ ,  $p \leq 0.001$ ; PI5K,  $n = 13$ ,  $p = 0.001$ ). *C*, expression of WA has no effect on p75 delivery to the apical surface. Kinetics of p75 delivery were measured as described in the legend to Fig. 1. Similar results were obtained in three experiments. *D*, WA does not affect basolateral delivery of TGN-staged VSV-G. MDCK cells were co-infected with VSV-G, and control, WA- or W-expressing AVs. VSV-G delivery to the basolateral cell surface was determined by cell surface biotinylation. Each experiment was performed using triplicate or quadruplicate samples, and mean  $\pm$  S.E. from the indicated number of experiments is plotted. Data for control at 0 and 60 min are the same as those shown in Fig. 1D. \* denotes significant difference from control at 0 min (control at 0 min,  $n = 3$ ; control at 60 min,  $n = 8$ ,  $p = 0.02$ ; WA,  $n = 7$ ,  $p = 0.005$ ; W,  $n = 7$ ,  $p = 0.03$ ; PI5K,  $n = 4$ ,  $p = 0.03$ ).

shown). Moreover, neither tight junction morphology nor the positioning and morphology of the Golgi complex was affected by expression of these constructs (Fig. 4, *C* and *D*), although we did notice in cells expressing very high levels of WA that the Golgi appeared to be somewhat dispersed toward the edges of the cells. Interestingly, whereas WA was diffusely expressed throughout the cytoplasm of polarized MDCK cells as expected, PI5K was concentrated near the apical membrane, a region that contains the supranuclear Golgi complex and the actin-rich terminal web of these cells (Fig. 4C).

We next assessed the impact of W or WA domain expression on early transport of HA through the biosynthetic pathway by monitoring the kinetics of HA acquisition of endo H resistance. Expression of WA or W had no discernable effects on the kinetics of HA traffic through the early Golgi (data not shown). Next, we examined the effects of these domains on HA delivery from the TGN to the plasma membrane. Expression of WA inhibited kinetics of HA delivery to the apical cell surface by approximately ~50–75% relative to control over a 60-min chase period (Fig. 5, *A* and *B*). Expression of the W domain did not significantly alter the delivery of HA indicating that expression of WA was not generally disrupting actin-driven processes. As with PI5K expression, the effect of WA on HA delivery was on rate rather than sorting, as HA surface polarity measured after long chase times was not compromised (not shown). The stimulatory and inhibitory effects of PI5K and WA on HA delivery kinetics were highly reproducible, and were statistically significant as assessed by Student's *t* test analysis of multiple experiments (Fig.

5B). The inhibitory effect of the WA domain was specific for lipid raft-enriched apical cargo, as there was no effect of the domain on the apical delivery of p75 (Fig. 5C). Moreover, expression of WA had no effect on the delivery of a basolateral marker, VSV-G (Fig. 5D).

**HA Is Associated with Actin Comets in MDCK Cells**—The data described above suggested the selective involvement of PI5K-stimulated, Arp2/3-dependent actin comets in the TGN to apical membrane delivery of HA. To test whether newly synthesized HA could be visualized in association with actin comets, MDCK cells seeded on glass coverslips were co-infected with AV-PI5K and AV-HA for 8 h, and then incubated at 19 °C for 2.5 h to accumulate HA in the TGN. Samples were then warmed to 37 °C for 30 min, fixed, and processed for indirect immunofluorescence to visualize actin, HA, and PI5K (Fig. 6). Numerous actin comets were detected in these cells, many of which stained positively for both PI5K and HA (Fig. 6, *arrows*). In 25 images we observed 71 comets of which 20 (28%) were positive for both HA and PI5K. By contrast, in 20 images we observed 57 comets of which only 2 (3.5%) were positive for p75 and PI5K. Together with our biochemical data, these studies provide strong evidence of a novel role for actin comets in polarized biosynthetic delivery of lipid raft-associated proteins.

**Efficient Apical Delivery of HA Requires Intact Actin and Microtubule Networks**—The selective requirement for Arp2/3 in cell surface delivery of HA delivery suggests a role for actin dynamics in apical membrane traffic. Indeed, depolymerization of actin filaments with cytochalasin D

## Actin Comet-mediated Apical Transport

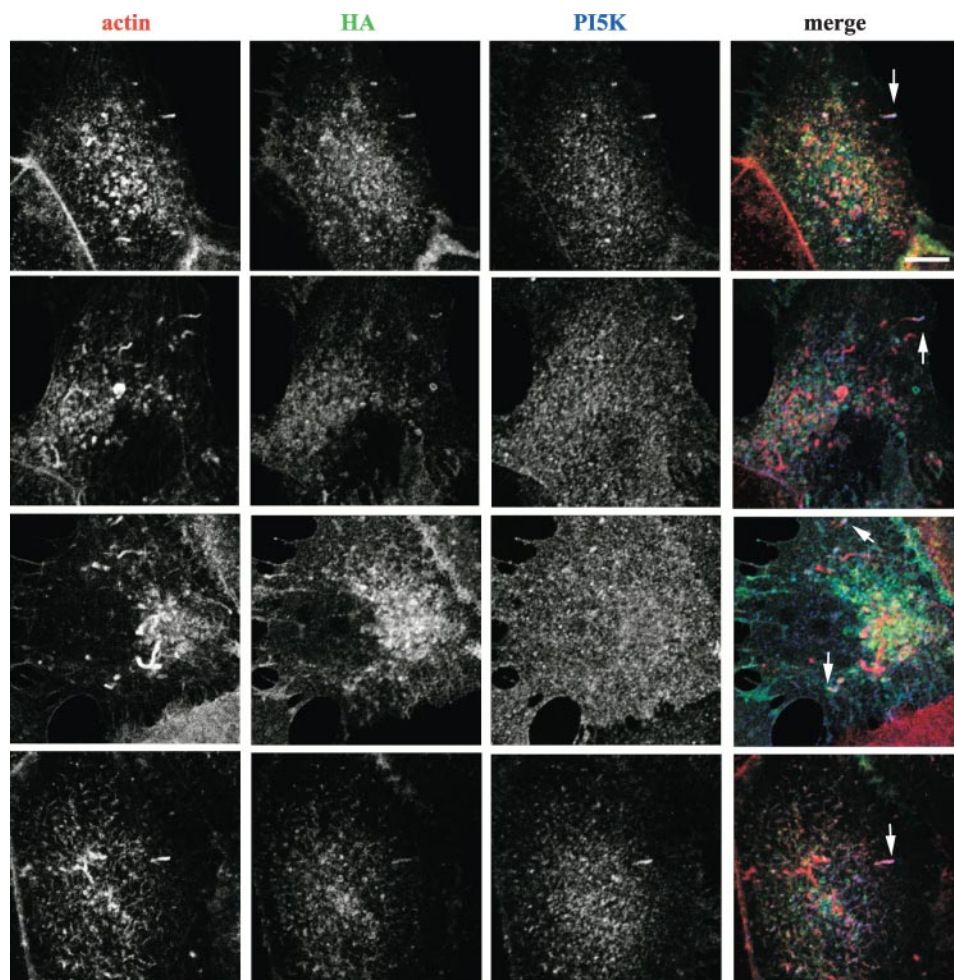


**FIGURE 6. HA and PI5K are associated with actin comets in MDCK cells.** MDCK cells grown on coverslips were co-infected with AV-HA and either control or PI5K for 8 h. HA was staged in the TGN for 2.5 h and 19 °C, then warmed to 37 °C for 30 min prior to fixation and processing for indirect immunofluorescence. Actin was stained using rhodamine phalloidin; HA was visualized using monoclonal antibody Fc125 followed by a Alexa 488-conjugated goat anti-mouse, and the PI5K HA epitope tag was visualized using a polyclonal antibody followed by Alexa 647-conjugated goat anti-rabbit. Individual confocal sections for each channel and a merged image demonstrating several examples of actin comets that co-label with HA and PI5K (marked with arrows) are shown. Scale bar, 7.5  $\mu$ m.

resulted in dramatic inhibition of HA surface delivery as expected, but also had profound effects on the polarity of HA delivery, most likely due to global changes in actin cytoskeleton structure and cell morphology (data not shown). However, the actin network in and of itself cannot confer directionality of transport, and targeted movement of at least some apically destined transport carriers in polarized cells has previously been ascribed to microtubule-dependent mechanisms (30–34). Moreover, inhibition of Arp2/3 function and actin comet formation by the WA domain or 1-butanol treatment did not completely block HA surface delivery in polarized MDCK cells. We therefore examined whether Arp2/3 functions synergistically with the microtubule network to enable efficient and polarized delivery of HA. Polarized MDCK cells co-infected with AV-HA and either control or WA-expressing AVs were radiolabeled and chased at 19 °C for 2 h. Prior to warming, cells were pretreated with the microtubule-depolymerizing agent nocodazole and HA delivery was assayed after a 1-h chase (Fig. 7). As expected, expression of WA or treatment with nocodazole alone partially inhibited delivery of HA (Fig. 7), and at this relatively short chase time, the polarity of delivery was intact (not shown). Interestingly, the effect of jointly disrupting Arp2/3 function and microtubule structure was additive, resulting in a nearly total blockade in HA delivery to the apical membrane. The dramatic inhibition of apical delivery was maintained over longer chase periods (up to 4 h; not shown). Treatment with nocodazole (either alone or with WA) also inhibited delivery of HA to the basolateral surface as well (not shown). These data suggest that HA-containing transport carriers utilize both Arp2/3 and microtubule-

dependent mechanisms to reach the apical surface, and that ablation of both mechanisms together results in a profound disruption in transport.

### DISCUSSION

Here we have investigated the role of PIP<sub>2</sub> metabolism in polarized biosynthetic traffic. Expression of PI5K in polarized MDCK cells markedly stimulated TGN to apical delivery of the lipid raft-associated protein influenza HA, whereas overexpression of Ocr1 inhibited delivery. Delivery of the non-raft-associated apical protein p75 and the basolateral marker VSV-G were unaffected by PI5K. Overexpression of PI5K also caused a dramatic stimulation in actin comets that was blocked by inhibition of Arp2/3 function upon expression of the WA domain of Scar1. Importantly, expression of this domain also selectively slowed HA transport. Moreover, pharmacological stimulation of actin comet formation by the protein kinase C activator PMA or inhibition by 1-butanol had parallel effects on HA delivery. HA and PI5K were visualized in association with actin comets, confirming a role for Arp2/3-mediated comet formation in HA transport. Disruption of actin and microtubules together had a synergistic effect on apical transport, suggesting that the two cytoskeletal assemblies normally act in concert to direct efficient apical transport. Together, our data suggest that apical transport of raft-dependent and -independent cargo is differentially regulated, and that raft-dependent cargo are transported via a protein kinase C, PIP<sub>2</sub>- and Arp2/3-dependent pathway consistent with the involvement of actin comets.

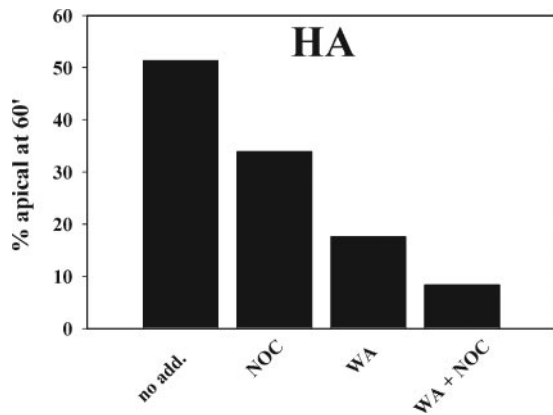


**FIGURE 7. The effects of WA and nocodazole on HA delivery are additive.** MDCK cells were co-infected with AV-HA and either control or WA-expressing AVs. Samples were starved, radiolabeled for 15 min, and chased 2 h at 19 °C. Samples were then incubated with 20  $\mu$ M nocodazole (NOC) or vehicle alone for 1 h on ice prior to warming to 37 °C for 1 h in the presence or absence of drug. HA delivery to the cell surface was quantitated by cell surface trypsinization.

**Role of Actin in Biosynthetic Traffic**—Numerous studies have documented the roles of actin in intra- and post-Golgi transport (35). These have ranged from observations of the presence of actin and actin-associated proteins associated with the Golgi complex (36–38) to more mechanistic insights into the potential roles of actin polymerization in biosynthetic traffic (39). Interestingly, the ADP-ribosylation factor ARF1 appears to be important for actin assembly on Golgi membranes (37) and this process requires coatomer-bound cdc42 and activation of the Arp2/3 complex (40, 41). Cdc42 may also regulate recruitment of dynein to coatomer protein complex I vesicles (42). However, the consequences of these signaling cascades on intra-Golgi membrane traffic are not clear. We found no effect of expression of either PI5K or the WA domain of Scar1 on intra-Golgi transport kinetics, suggesting that PIP<sub>2</sub>- and Arp2/3-mediated actin polymerization are not required for the transport or maturation of cargo.

ARF-dependent actin recruitment has also been implicated in post-Golgi transport. Recruitment to Golgi membranes of the actin-binding protein cortactin was shown to be ARF-dependent, and disruption of this complex in BHK cells had profound effects on the surface delivery of VSV-G without affecting intra-Golgi transport (43). However, our laboratory has previously demonstrated that TGN export of HA occurs independently of ARF function (44). Modulation of actin dynamics by the clathrin- and actin-binding protein Hip1R has also been suggested to regulate formation and release of clathrin-coated vesicles from the TGN (45).

**Actin and Polarized Membrane Traffic**—Specific roles for actin polymerization in the transport of apical proteins, and lipid raft-associated cargo in particular, have previously been suggested. Rozelle *et al.* (18) observed that newly synthesized HA was preferentially localized to the tips of short polymers of actin reminiscent of N-WASP-dependent comets in PI5K-overexpressing cells. In support of this, PIP<sub>2</sub> has been suggested to be enriched in lipid rafts (46–48) although this conclusion has recently been challenged (49, 50). Moreover, our observation that expression of either PI5K or WA had no effect on apical delivery of a non-raft-associated protein adds support to the idea that transport of raft-associated and raft-independent proteins is differentially regulated. Jacob *et al.* (3, 4) have previously suggested that biosynthetic transport carriers containing the lipid raft-associated hydrolase sucrase isomaltase traffic via actin cables to the cell surface, whereas carriers enriched in the non-raft apical protein lactase-phlorizin hydrolase traffic in separate carriers in an actin-independent manner. Recently, the same group identified  $\alpha$ -kinase 1, which phosphorylates the motor protein myosin I, as a component of sucrase isomaltase but not lactase-phlorizin

hydrolase-containing vesicles and demonstrated a role for this motor in apical delivery of sucrase isomaltase (51). Whether  $\alpha$ -kinase 1 activity is important for the PI5K-mediated stimulation of HA delivery we observed is not known; however, in a parallel scenario, both myosin motors and N-WASP-Arp2/3-mediated actin polymerization have been suggested as mechanisms that propel internalized endocytic vesicles through the actin-rich cortical cytoskeleton (16, 52–55).

**Role of PIP<sub>2</sub> Metabolism in Apical Membrane Traffic**—What is the site of PI5K function in TGN to apical membrane delivery of HA? Whereas no PI5K isoform has been localized to the Golgi complex, the majority of this enzyme was associated with actin filaments near the apical surface of polarized MDCK cells close to the supranuclear Golgi complex. However, there are indications that some apically destined proteins may traverse endosomal intermediates *en route* to the cell surface (56–58), suggesting the possibility that the PI5K- and Ocr1-mediated effects on HA transport we observed might occur at post-TGN sites. Whereas the majority of Ocr1 is localized to the TGN (15), endosomal localization of Ocr1 has also been reported (59, 60) and Lowe syndrome fibroblasts exhibit dramatically increased numbers of actin comets compared with normal fibroblasts (61, 62).

**Relationship between PI4P and PIP<sub>2</sub> Synthesis in Polarized Biosynthetic Traffic**—Previously we found that overexpression of wild type PI4KIII $\beta$  or expression of frequenin/NCS-1, which stimulates PI4KIII $\beta$  activity, inhibited apical delivery kinetics of HA, suggesting a negative regulatory role for PI4P in TGN to apical membrane transport (8, 63). A selective role in apical membrane traffic for the PI4P-binding protein Fapp2 has also been demonstrated (64). Our observation here that overexpression of PI5K stimulates apical delivery is at odds with a simplistic precursor-product view of phosphatidylinositol metabolism in which changes in PI4P lead to parallel changes in PIP<sub>2</sub>. Indeed, we have previously found that PI4KIII $\beta$ -mediated increases in cellular PI4P levels do not affect PIP<sub>2</sub> levels (8). It is possible that PI5K-mediated conversion of PI4P to PIP<sub>2</sub> might stimulate membrane traffic by relieving the inhibitory effect of PI4P; however, this is unlikely given the high levels of PI4P in the Golgi complex relative to PIP<sub>2</sub>. It is also possible that overexpression of PI5K causes localized changes in PI4P distribution; however, a more likely scenario is that PI4P and PIP<sub>2</sub> function independently to modulate distinct steps in membrane transport.

**Concerted Cytoskeletal Function in Polarized Membrane Traffic**—Regardless of the role(s) for actin polymerization in apical membrane traffic, it is likely that the long-range directionality of biosynthetic membrane traffic is provided ultimately by the microtubule network. Previous biochemical studies have demonstrated a role for microtubules in polarized membrane transport in MDCK cells (31, 32, 65, 66). In addition, live cell imaging has clearly shown that VSV-G-containing transport carriers move to the plasma membrane on microtubule tracks (67, 68). We found that disruption of actin with cytochalasin D (not shown) or by expression of WA in concert with nocodazole treatment virtually abolished delivery of HA to the apical membrane, and ultimately disrupted the polarity of delivery. In contrast, expression of WA alone had no effect on HA polarity. Our data are reminiscent of studies by Maples *et al.* (69) who demonstrated a concerted role for actin and microtubules in basolateral to apical transcytosis of the polymeric immunoglobulin receptor. Our results do not necessarily suggest that actin comets are obligatory for apical delivery, but rather that they may facilitate apical transport of HA under some conditions. We hypothesize that actin-based movement of HA-containing transport carriers facilitates their access to microtubule tracks that provide the directionality for efficient transport to the apical mem-

## Actin Comet-mediated Apical Transport

brane, and/or ferries transport carriers across the actin-rich terminal web to their site of fusion.

*Acknowledgments*—We thank Robert Nussbaum, Sharon Suchy, James Casanova, Dorothy Schafer, Christopher Carpenter, Andreas Jeromin, Anne Musch, Enrique Rodriguez-Boulan, and Moses Chao for their generous gifts of cDNA constructs and recombinant adenoviruses.

### REFERENCES

- Schuck, S., and Simons, K. (2004) *J. Cell Sci.* **117**, 5955–5964
- Rodriguez-Boulan, E., Kreitzer, G., and Musch, A. (2005) *Nat. Rev. Mol. Cell Biol.* **6**, 233–247
- Jacob, R., and Naim, H. (2001) *Curr. Biol.* **11**, 1444–1450
- Jacob, R., Heine, M., Alfalah, M., and Naim, H. Y. (2003) *Curr. Biol.* **13**, 607–612
- Roth, M. G. (2004) *Physiol. Rev.* **84**, 699–730
- Wei, Y. J., Sun, H. Q., Yamamoto, M., Wlodarski, P., Kunii, K., Martinez, M., Barylko, B., Albanesi, J. P., and Yin, H. L. (2002) *J. Biol. Chem.* **277**, 46586–46593
- Godi, A., Pertile, P., Meyers, R., Marra, P., Di Tullio, G., Iurisci, C., Luini, A., Corda, D., and De Matteis, M. A. (1999) *Nat. Cell Biol.* **1**, 280–287
- Bruns, J. R., Ellis, M. A., Jeromin, A., and Weisz, O. A. (2001) *J. Biol. Chem.* **277**, 2012–2018
- Weixel, K. M., Blumental-Perry, A., Watkins, S. C., Aridor, M., and Weisz, O. A. (2005) *J. Biol. Chem.* **280**, 10501–10508
- Watt, S. A., Kular, G., Fleming, I. N., Downes, C. P., and Lucocq, J. M. (2002) *Biochem. J.* **363**, 657–666
- Jones, D. H., Morris, J. B., Morgan, C. P., Kondo, H., Irvine, R. F., and Cockcroft, S. (2000) *J. Biol. Chem.* **275**, 13962–13966
- Lorra, C., and Huttner, W. B. (1999) *Nat. Cell Biol.* **1**, E113–E115
- Huijbregts, R. P., Topalof, L., and Bankaitis, V. A. (2000) *Traffic* **1**, 195–202
- Dressman, M. A., Olivos-Glander, I. M., Nussbaum, R. L., and Suchy, S. F. (2000) *J. Histochem. Cytochem.* **48**, 179–190
- Olivos-Glander, I. M., Janne, P. A., and Nussbaum, R. L. (1995) *Am. J. Hum. Genet.* **57**, 817–823
- Taunton, J., Rowning, B. A., Coughlin, M. L., Wu, M., Moon, R. T., Mitchison, T. J., and Larabell, C. A. (2000) *J. Cell Biol.* **148**, 519–530
- Miki, H., Miura, K., and Takenawa, T. (1996) *EMBO J.* **15**, 5326–5335
- Rozelle, A. L., Machesky, L. M., Yamamoto, M., Driessens, M. H., Insall, R. H., Roth, M. G., Luby-Phelps, K., Marriott, G., Hall, A., and Yin, H. L. (2000) *Curr. Biol.* **10**, 311–320
- Henkel, J. R., Apodaca, G., Altschuler, Y., Hardy, S., and Weisz, O. A. (1998) *Mol. Biol. Cell* **8**, 2477–2490
- Apodaca, G., Katz, L. A., and Mostov, K. E. (1994) *J. Cell Biol.* **125**, 67–86
- Henkel, J. R., Popovich, J. L., Gibson, G. A., Watkins, S. C., and Weisz, O. A. (1999) *J. Biol. Chem.* **274**, 9854–9860
- Altschuler, Y., Kinlough, C. L., Poland, P. A., Apodaca, G., Weisz, O. A., and Hughey, R. P. (1999) *Mol. Biol. Cell* **11**, 819–831
- Yeaman, C., Burdick, D., Muesch, A., and Rodriguez-Boulan, E. (1998) in *Cell Biology: A Laboratory Handbook* (Celis, J. E., ed) 2nd Ed., pp 237–245, Academic Press, San Diego
- Lefrancois, L., and Lyles, D. S. (1982) *Virology* **121**, 168–174
- Yang, S. A., Carpenter, C. L., and Abrams, C. S. (2004) *J. Biol. Chem.* **279**, 42331–42336
- Orth, J. D., Krueger, E. W., Cao, H., and McNiven, M. A. (2002) *Proc. Natl. Acad. Sci. U. S. A.* **99**, 167–172
- Lee, E., and De Camilli, P. (2002) *Proc. Natl. Acad. Sci. U. S. A.* **99**, 161–166
- Chen, Y.-G., Siddhanta, A., Austin, C. D., Hammond, S. M., Sung, T.-C., Frohman, M. A., Morris, A. J., and Shields, D. (1997) *J. Cell Biol.* **138**, 495–504
- Machesky, L. M., and Insall, R. H. (1998) *Curr. Biol.* **8**, 1347–1356
- Noda, Y., Okada, Y., Saito, N., Setou, M., Xu, Y., Zhang, Z., and Hirokawa, N. (2001) *J. Cell Biol.* **155**, 77–88
- Parczyk, K., Haase, W., and Kondor-Koch, C. (1989) *J. Biol. Chem.* **264**, 16837–16846
- Grindstaff, K. K., Bacallao, R. L., and Nelson, W. J. (1998) *Mol. Biol. Cell* **9**, 685–699
- Rindler, M. J., Ivanov, I. E., and Sabatini, D. D. (1987) *J. Cell Biol.* **104**, 231–241
- Kreitzer, G., Marmorstein, A., Okamoto, P., Vallee, R., and Rodriguez-Boulan, E. (2000) *Nat. Cell Biol.* **2**, 125–127
- Allan, V. J., Thompson, H. M., and McNiven, M. A. (2002) *Nat. Cell Biol.* **4**, E236–E242
- Heimann, K., Percival, J. M., Weinberger, R., Gunning, P., and Stow, J. L. (1999) *J. Biol. Chem.* **274**, 10743–10750
- Fucini, R. V., Navarrete, A., Vadakkan, C., Lacomis, L., Erdjument-Bromage, H., Tempst, P., and Stamnes, M. (2000) *J. Biol. Chem.* **275**, 18824–18829
- Matas, O. B., Martinez-Menarguez, J. A., and Egea, G. (2004) *Traffic* **5**, 838–846
- Stamnes, M. (2002) *Curr. Opin. Cell Biol.* **14**, 428–433
- Fucini, R. V., Chen, J. L., Sharma, C., Kessels, M. M., and Stamnes, M. (2002) *Mol. Biol. Cell* **13**, 621–631
- Dubois, T., Paleotti, O., Mironov, A. A., Fraiser, V., Stradal, T. E., De Matteis, M. A., Franco, M., and Chavrier, P. (2005) *Nat. Cell Biol.* **7**, 353–364
- Chen, J. L., Fucini, R. V., Lacomis, L., Erdjument-Bromage, H., Tempst, P., and Stamnes, M. (2005) *J. Cell Biol.* **169**, 383–389
- Cao, H., Weller, S., Orth, J. D., Chen, J., Huang, B., Chen, J. L., Stamnes, M., and McNiven, M. A. (2005) *Nat. Cell Biol.* **7**, 483–492
- Ellis, M. A., Miedel, M. T., Guerriero, C. J., and Weisz, O. A. (2004) *J. Biol. Chem.* **279**, 52735–52743
- Carreno, S., Engqvist-Goldstein, A. E., Zhang, C. X., McDonald, K. L., and Drubin, D. G. (2004) *J. Cell Biol.* **165**, 781–788
- Hope, H. R., and Pike, L. J. (1996) *Mol. Biol. Cell* **7**, 843–851
- Laux, T., Fukami, K., Thelen, M., Golub, T., Frey, D., and Caroni, P. (2000) *J. Cell Biol.* **149**, 1455–1471
- Caroni, P. (2001) *EMBO J.* **20**, 4332–4336
- van Rhee, J., Achame, E. M., Janssen, H., Calafat, J., and Jalink, K. (2005) *EMBO J.* **24**, 1664–1673
- Brough, D., Bhatti, F., and Irvine, R. F. (2005) *J. Cell Sci.* **118**, 3019–3025
- Heine, M., Cramm-Behrens, C. I., Ansari, A., Chu, H. P., Ryazanov, A. G., Naim, H. Y., and Jacob, R. (2005) *J. Biol. Chem.* **280**, 25637–25643
- Morris, S. M., Arden, S. D., Roberts, R. C., Kendrick-Jones, J., Cooper, J. A., Luzio, J. P., and Buss, F. (2002) *Traffic* **3**, 331–341
- Benesch, S., Polo, S., Lai, F. P., Anderson, K. I., Stradal, T. E., Wehland, J., and Rottner, K. (2005) *J. Cell Sci.* **118**, 3103–3115
- Merrifield, C. J., Qualmann, B., Kessels, M. M., and Almers, W. (2004) *Eur. J. Cell Biol.* **83**, 13–18
- Merrifield, C. J. (2004) *Trends Cell Biol.* **14**, 352–358
- Ang, A. L., Taguchi, T., Francis, S., Folsch, H., Murrells, L. J., Pypaert, M., Warren, G., and Mellman, I. (2004) *J. Cell Biol.* **167**, 531–543
- Orzech, E., Cohen, S., Weiss, A., and Aroeti, B. (2000) *J. Biol. Chem.* **275**, 15207–15219
- Polishchuk, R., Di Pentima, A., and Lippincott-Schwartz, J. (2004) *Nat. Cell Biol.* **6**, 297–307
- Choudhury, R., Diao, A., Zhang, F., Eisenberg, E., Saint-Pol, A., Williams, C., Konstantakopoulos, A., Lucocq, J., Johannes, L., Rabouille, C., Greene, L. E., and Lowe, M. (2005) *Mol. Biol. Cell* **16**, 3467–3479
- Ungewickell, A., Ward, M. E., Ungewickell, E., and Majerus, P. W. (2004) *Proc. Natl. Acad. Sci. U. S. A.* **101**, 13501–13506
- Suchy, S. F., and Nussbaum, R. L. (2002) *Am. J. Hum. Genet.* **71**, 1420–1427
- Allen, P. G. (2003) *Nat. Cell Biol.* **5**, 972–979
- Weisz, O. A., Gibson, G. A., Leung, S.-M., Roder, J., and Jeromin, A. (2000) *J. Biol. Chem.* **275**, 24341–24347
- Vieira, O. V., Verkade, P., Manninen, A., and Simons, K. (2005) *J. Cell Biol.* **170**, 521–526
- Boll, W., Partin, J. S., Katz, A. I., Caplan, M. J., and Jamieson, J. D. (1991) *Proc. Natl. Acad. Sci. U. S. A.* **88**, 8592–8596
- Breitfeld, P. P., McKinnon, W. C., and Mostov, K. E. (1990) *J. Cell Biol.* **111**, 2365–2373
- Hirschberg, K., Miller, C. M., Ellenberg, J., Presley, J. F., Siggia, E. D., Phair, R. D., and Lippincott-Schwartz, J. (1998) *J. Cell Biol.* **143**, 1485–1503
- Toomre, D., Keller, P., White, J., Olivo, J. C., and Simons, K. (1999) *J. Cell Sci.* **112**, 21–33
- Maples, C. J., Ruiz, W. G., and Apodaca, G. (1996) *J. Biol. Chem.* **272**, 6741–6751